The temperature-signaling cascade in sponges involves a heat-gated cation channel, abscisic acid, and cyclic ADP-ribose

Elena Zocchi*†, Armando Carpaneto‡, Carlo Cerrano§, Giorgio Bavestrello¶, Marco Giovine*, Santina Bruzzone*, Lucrezia Guida*, Luisa Franco*, and Cesare Usai‡

*Dipartimento di Medicina Sperimentale, Sezione Biochimica, University of Genova, Viale Benedetto XV no. 1, 16132 Genova, Italy; ‡Institute of Cybernetics and Biophysics, National Research Council, Via De Marini 6, 16149 Genova, Italy; §Dipartimento per lo Studio del Territorio e sue Risorse, University of Genova, Corso Europa 26, 16132 Genova, Italy; and ¶Istituto di Scienze del Mare, University of Ancona, Via Brecce Bianche, 60131 Ancona, Italy

Edited by Michael J. Berridge, The Babraham Institute, Cambridge, United Kingdom, and approved October 17, 2001 (received for review August 22, 2001)

Sponges (phylum Porifera) are the phylogenetically oldest metazoan animals, their evolution dating back to 600 million years ago. Here we demonstrate that sponges express ADP-ribosyl cyclase activity, which converts NAD^+ into cyclic ADP-ribose, a potent and universal intracellular Ca^{2+} mobilizer. In *Axinella polypoides* (Demospongiae, Axinellidae), ADP-ribosyl cyclase was activated by temperature increases by means of an abscisic acid-induced, protein kinase A-dependent mechanism. The thermosensor triggering this signaling cascade was a heat-activated cation channel. Elucidation of the complete thermosensing pathway in sponges highlights a number of features conserved in higher organisms: (*i*) the cation channel thermoreceptor, sensitive to heat, mechanical stress, phosphorylation, and anesthetics, shares all of the functional characteristics of the mammalian heat-activated background K^+ channel responsible for central and peripheral thermosensing; (*ii*) involvement of the phytohormone abscisic acid and cyclic ADP-ribose as its second messenger is reminiscent of the drought stress signaling pathway in plants. These results suggest an ancient evolutionary origin of this stress-signaling cascade in a common precursor of modern Metazoa and Metaphyta.

ADP-ribosyl cyclase activity is expressed along the phylogenetic tree from unicellular protists (1) to mammals (2). It converts NAD^+ to cyclic ADP-ribose (cADPR) (3), an intracellular calcium mobilizer that is being increasingly recognized as a pivotal signaling molecule, involved in such diverse functions as cell cycle regulation (1) (protists), oocyte fertilization (4) (invertebrates), insulin secretion (5), and cell proliferation (6) (mammals). The peculiar position of Porifera in the phylogenetic tree [they are the oldest known Metazoa, sharing a common ancestor with all multicellular animals (7)] and the presence of signaling pathways in these organisms (8) prompted us to investigate the presence, and the functional role, of the ADP-ribosyl cyclase/cADPR system in marine sponges.

Materials and Methods

Sponges. Sponges were collected in the Ligurian Sea (Mediterranean Sea), at Gallinara Island (Genova, Italy) at a depth between 35 and 45 m. The temperature was maintained at 14°C during transfer of the animals to the lab. They were kept in an aquarium in natural seawater (SW) at 14°C for 5–7 days before utilization. All procedures involving sponge tissue were performed at 14°C. As the most ancient and simple metazoan animals, sponges lack a defined tissue organization. Cells are embedded in a collagenous matrix, impregnated with siliceous or calcareous spicules, surrounding a complex network of internal canals, through which water circulates. Intact sponge cells ($\approx$8 μm diameter) could be easily obtained by gentle squeezing of cleanly cut *Axinella polypoides* fragments. Cell viability, as checked microscopically, was always $\geq$95% after mechanical dissociation and after exposure of the cells to heat stress or abscisic acid (ABA).

HPLC and Fluorimetric Assays of Enzymatic Activities. Sponges were cut into small pieces, and cells were dissociated mechanically (9) and washed once by sedimentation in SW. Intact cells or cell lysates, obtained by addition of 0.01% Triton X-100 and brief (6 s) sonication, were diluted in SW to $\approx$0.1 and 0.01 mg protein/ml, respectively, and were incubated at 14°C in SW in the presence of 0.2 mM NAD^+, nicotinamide guanine dinucleotide, or cADPR for determination of ADP-ribosyl cyclase, GDP-ribosyl cyclase, and cADPR hydrolase activities, respectively. At various times, aliquots were withdrawn and briefly centrifuged, and the supernatant was trichloroacetic acid-extracted and analyzed by HPLC (10). The effect of a brief (less than 5 min) exposure of *A. polypoides* cells to various conditions affecting cyclase activity also was investigated by microfluorimetric detection of fluorescent cyclic inosine diphosphate ribose produced from nicotinamide hypoxanthine dinucleotide (NHD^+) (11). Briefly, intact cells were resuspended in SW and exposed to the various treatments (heat stress or chemicals) at the selected temperature (26°C or 14°C) in a water bath. Thereafter, cells were diluted 200 times in SW at 14°C containing 0.01% Triton X-100 and briefly sonicated, and cyclase activity was measured in a 2-ml cuvette after addition of 0.2 mM NHD^+ in a thermostated (14°C) fluorimeter (Perkin–Elmer) with λ_{ex} = 200 nm and λ_{em} = 490 nm. The slope of the linear fluorescence increase of treated samples was compared with that of controls.

Calcium Measurements. Freshly dissociated *A. polypoides* cells were incubated in the dark at 14°C in calcium-, magnesium-free SW (CMF-SW) in the presence of 10 μM Fura 2-AM (Calbiochem) for 90 min. Cells were washed once (3,000 $\times$ *g* for 10 s) in CMF-SW, resuspended in the same solution containing 10 mM glucose, and placed in a thermostated, 2 ml-cuvette under continuous slow stirring, and the E340/E380 nm fluorescence ratio was determined with a microfluorimetric detector (Cairn, Faversham, U.K.) (6). EGTA-AM loading of the cells, when needed, was performed before the Fura loading. Cells were incubated at 14°C for 30 min with 20 μM EGTA-AM (Calbiochem), and 10 μM Fura 2-AM was then added for further 90-min incubation.

Sponge Cell Permeabilization. Fura 2-loaded sponge cells were resuspended in CMF-SW in the presence of 25 μM EGTA, this concentration being sufficient to chelate contaminant calcium.

This paper was submitted directly (Track II) to the PNAS office.

Abbreviations: cADPR, cyclic ADP-ribose; SW, seawater; CMF-SW, calcium-, magnesium-free SW; ABA, abscisic acid; NHD^+, nicotinamide hypoxanthine dinucleotide; AA, arachidonic acid; PKA, protein kinase A; $[Ca^{2+}]_i$, intracellular Ca^{2+} concentration; 8-Br-cADPR, 8-bromo-cADPR.

†To whom reprint requests should be addressed. E-mail: ezocchi@unige.it.

The publication costs of this article were defrayed in part by page charge payment. This article must therefore be hereby marked "*advertisement*" in accordance with 18 U.S.C. §1734 solely to indicate this fact.

BIOCHEMISTRY

Aliquots of 200 μl cell suspension were placed in a thermostated cuvette at 14°C under continuous, slow stirring, and the following detergents were added sequentially: 0.004% Triton X-100 reduced form (nonfluorescent, suitable for fluorimetric assays, from Fluka), 2 μM digitonin (Sigma), and 0.1 mg/ml saponin (Sigma). Cells were incubated for 10–15 min before addition of 10 μM cADPR or ryanodine.

cADPR Detection. The intracellular cADPR concentration was determined by HPLC analysis on neutralized trichloroacetic acid cell extracts, as described (12, 13).

ABA Detection. Freshly cut *A. polypoides* fragments were homogenized in 6 vol of methanol/water (80:20 vol/vol), methanol was evaporated, and the aqueous extract was acidified at pH 3.1 with trifluoroacetic acid and extracted with diethylether (14). After removal of diethylether under vacuum the extract was redissolved in water and subjected to HPLC analysis or ELISA.

HPLC analysis. Preparative and analytical chromatographies were performed on a Hewlett–Packard 1090 instrument equipped with DAD detector. The extract from 40 g of sponge tissue was injected into a preparative (10 × 250 mm) C18 reverse-phase column (Bio-Rad): buffer A was water containing 0.01% trifluoroacetic acid (TFA), buffer B was 70% methanol in water containing 0.01% TFA. The gradient was from 100% A to 100% B in 60 min at a flow rate of 2 ml/min. At the elution time of standard ABA fractions were collected, dried in a Rotovapor, redissolved in water, and injected into an analytical (10 × 4.6 mm) ODS-Hypersil C18 column (Hewlett–Packard): buffer A was water containing 0.01% TFA, buffer B was 50% acetonitrile in water containing 0.01% TFA. The gradient was from 100% A to 70% B in 120 min, at a flow rate of 0.4 ml/min. ABA eluted as a sharp peak at 90 min retention time. Absorbance spectrum, retention time, and peak area of sample ABA were compared with those of a computer-stored standard, allowing both identification and quantitation of the hormone. Fractions of the analytical HPLC containing ABA were dried, redissolved in Tris-buffered saline, pH 7.4, and subjected to ELISA to confirm identification and quantitation.

ELISA. The extracts from 2 g of sponge tissue, or HPLC fractions containing purified ABA, were assayed with a competitive ELISA assay kit (Agdia, Elkhart, IN) according to the manufacturer's instructions.

Immunopurification of Phosphorylated Cyclase and Detection on SDS/PAGE. Sponge fragments (≈1 g) were incubated in phosphate-free artificial SW for 12 h at 14°C in the presence of 5 μCi/ml of [^{32}P]-orthophosphate (285 Ci/mg, NEN Life Science Products). Fragments were then rinsed in SW and subjected to the various treatments (incubation at 14°C or 28°C or at 14°C in the presence of 50 nM ABA with or without 1 μM K252a) for 5 min. Thereafter, cells were mechanically dissociated, lysed by sonication in ice in the presence of protease and phosphatase inhibitors (Sigma) and then centrifuged at 50,000 × *g* for 10 min. The supernatants were recovered, and 0.1% SDS was added to mildly denature proteins and improve antibody binding to phosphoserines (15). Lysates were incubated with 50 μl antiphosphoserine antibody-coated agarose (Sigma) for 2 h at 5°C. The resin was recovered by centrifugation, washed four times in 10 mM Hepes, pH 7.5, containing 0.1% SDS, protease, and phosphatase inhibitors, and bound proteins were eluted with 1 mM phosphoserine. Eluates were heated at 50°C for 3 min in the presence of a modified 4× Laemmli sample buffer, containing 1.5% SDS (instead of the usual 8%) and no β-mercaptoethanol, and were run on SDS/PAGE (15% polyacrylamide). The gel was washed in 10 mM Tris·HCl, pH 8.8, for 30 min with repeated buffer changes to remove excess SDS; 0.2 mM NHD^+ was then added and after 10 min incubation in the dark at 20°C the fluorescent bands, corresponding to locally produced cyclic inosine diphosphate ribose, were visualized under UV light with a Bio-Rad Chemi Doc instrument. Finally, the gel was dried and autoradiographed, and radioactive bands were detected with a Packard Cyclone detector.

$^{86}Rb^+$ Efflux. The method was adapted from ref. 16 with some modifications, aimed at minimizing the mechanical stress on the cells during efflux measurements. Mechanically dissociated *A. polypoides* cells were loaded with $^{86}Rb^+$ by incubation at 14°C for 3 h in the presence of 1 μCi/ml $^{86}Rb^+$ (NEN Life Science Products) in SW. The supernatant, containing most of the radioactivity, was then removed from the sedimented cells and cells were washed four times (3,000 × *g* for 10 s) in 1 ml SW. Cells were resuspended in SW and 0.4 ml of the suspension was placed in 0.45 μm (micropure) Amicon separators, which in turn were inserted into Eppendorf tubes, containing 1 ml SW each, at the desired temperature. This set-up enabled measurement of the radioactivity released from the cells (and diffused through the filter into the Eppendorf tube) without the need to centrifuge the cells at each time point to separate them from the medium. At 10-min intervals the separators were transferred to a fresh tube. The radioactivity of the SW in the Eppendorf tubes was determined in a Packard β-counter after addition of 20 ml scintillation liquid.

Electrophysiology. The experimental setting for electrophysiological measurements has been described in detail (17). Briefly, cells were dissociated by gentle suction at the surface of a clean cut of the sponge branches and put into the perfusion chamber in artificial SW. The presence in the bathing solution of trivalent cations (Gd^{3+} or La^{3+}, 100 ÷ 300 μM) was essential to seal the electrode to the cell membrane, but, after the gigaseal formation, they were washed out without affecting the seal resistance. The different solutions were administered by a superfusion pipette located very near to the recorded cell, and their temperature was continuously monitored. The artificial SW solution contained 450 mM NaCl, 10 mM KCl, 50 mM $MgCl_2$, 10 mM $CaCl_2$, 20 mM Hepes (pH 7.9, with NaOH ≈14 mM). In whole-cell experiments the pipette solution (IntA) contained 10 mM NaCl, 150 mM KCl, 5 mM $MgCl_2$, 10 μM $CaCl_2$, 20 mM Hepes, 785 mM sorbitol (pH 7.2, with KOH ≈8 mM), and in cell-attached experiments the pipette solution (IntB) contained 450 mM NaCl, 10 mM KCl, 20 mM Tris·MES, 180 mM sorbitol (pH 7.9). Stock solutions of arachidonic acid (AA) (100 mM) in ethanol were stored at −20°C. Data analysis was done by custom-made programs using IGOR (Wavemetrics, Lake Oswego, OR).

Results and Discussion

ADP-Ribosyl Cyclase Activity in Sponges. ADP-ribosyl cyclase activity was detected in cell lysates obtained from several different sponge genera, including demospongiae and calcispongiae (see Table 1, which is published as supporting information on the PNAS web site, www.pnas.org). Because several ADP-ribosyl cyclases are bifunctional enzymes, also expressing cADPR hydrolase activity (degrading cADPR to ADP-ribose), we also measured the hydrolase activity, which proved to be much lower than the cyclase. Specifically, the ratio between cyclase activity on NAD^+ and hydrolase activity on cADPR was always ≥100, similar to that of the invertebrate (*Aplysia*) cyclase (18) and ≈1,000 times higher than that of the mammalian enzyme (6). The sponges' cyclase activity on the natural substrate NAD^+ was higher than that recorded on the NAD^+ analog nicotinamide guanine dinucleotide, as observed for the invertebrate enzyme (18). In all species tested, cyclase and cADPR hydrolase activities were approximately 2-fold higher in cell lysates over levels measured on intact cells, except in *A. polypoides*, where the ratio between total and ectocellular cyclase activity was ≈14. Thus, ectocellular as well as intracellular cyclase activity is present in sponges, similarly to what has been observed in sea urchin eggs (19).

A. polypoides, an arborescent sponge living on coralligenous or detritic bottoms, expressed by far the highest cyclase activity

among the species tested. Its ectocyclase of 107 ± 25 nmol cADPR/min per mg protein, as measured on intact cells, is ≈500 times higher than the ectocyclase activity expressed by cyclase-positive mammalian cells (6).

The known calcium-releasing activity of the product of ADP-ribosyl cyclase, cADPR, which acts by binding to a microsomal receptor/Ca^{2+} channel known as the ryanodine receptor (2), prompted us to investigate the responsiveness of permeabilized *A. polypoides* cells to the cyclic nucleotide and ryanodine. Indeed, in permeabilized *A. polypoides* cells, both cADPR and ryanodine induced an immediate and similar calcium release (see Fig. 4 *A* and *B*, which is published as supporting information on the PNAS web site). Addition of ryanodine after cADPR was ineffective, confirming that calcium release occurred from the same stores for both molecules (2). Pretreatment of the permeabilized cells with the cADPR antagonist 8-bromo-cADPR (8-Br-cADPR) before addition of cADPR completely abolished the calcium release (Fig. 4*C*), indicating that the observed response was indeed attributable to cADPR.

Thus, *A. polypoides* cells are competent in both production of and responsiveness to cADPR.

Heat Stress and ABA Induce Activation of ADP-Ribosyl Cyclase. Occasionally, specimens from the genus *Axinella* and *Petrosia* showed a much higher cyclase activity compared with mean recorded values, a result we tentatively attributed to the increased temperature to which they had been inadvertently exposed during transfer to the laboratory. Thus, we investigated the effect of temperature on the cyclase activity of *A. polypoides*.

Cyclase activity increased approximately 3-fold after even a brief exposure (2 min) of intact *A. polypoides* cells to an increased temperature (26°C instead of 14°C, the temperature at which animals were kept in the aquarium; see Fig. 5, white bars, which is published as supporting information on the PNAS web site). Similar results also were obtained with a microfluorimetric assay of cyclase activity based on the fluorescent properties of cyclic inosine diphosphate ribose, the product of the cyclase activity on deamino NAD^+ (NHD^+) (20). This set-up enabled a more accurate investigation of brief (<5 min) exposures of the cells to high temperature, confirming near-maximal (72%) activation of the cyclase after exposure of the cells to 26°C for as few as 60 s (not shown). The enhanced cyclase activity measured upon exposure of *A. polypoides* cells to 26°C was paralleled by a 7-fold increase of the intracellular cADPR concentration (from a basal value of 0.24 ± 0.06 nmol/mg protein to 0.9 ± 0.03, 1.58 ± 0.6 and 1.65 ± 0.6 nmol/mg after 5, 10 and 60 min, respectively; mean ± SD of three experiments).

The increase of $[cADPR]_i$ after heat stress in sponges was reminiscent of a similar effect induced by drought stress in plants, where the signaling pathway had been demonstrated to involve the phytohormone ABA (21). This finding prompted us to investigate the effect of ABA on sponge cyclase activity. An increase of cyclase activity also was observed upon incubation of *A. polypoides* cells in the presence of nanomolar ABA concentrations (see Fig. 5, shaded bars). The extent of the increase was comparable to that elicited by heat stress (Fig. 5, white bars). Maximal activation (4-fold increase over control) was observed with ABA concentrations ranging from 50 nM (Fig. 5) to 5 nM (not shown). The effects of short incubation times (<5 min) with ABA also were investigated with the microfluorimetric assay, which confirmed a near-maximal (75%) cyclase activation after a 60-s exposure of the intact cells to the hormone. Stimulation of cyclase activity by ABA (at concentrations ranging from 5 to 50 nM) was paralleled by an increase of the $[cADPR]_i$ similar in both extent and kinetics to that observed with the temperature stress (see above): no effect was observed for subnanomolar ABA concentrations, indicating a threshold concentration for cyclase activation in the nanomolar range (5–10 nM).

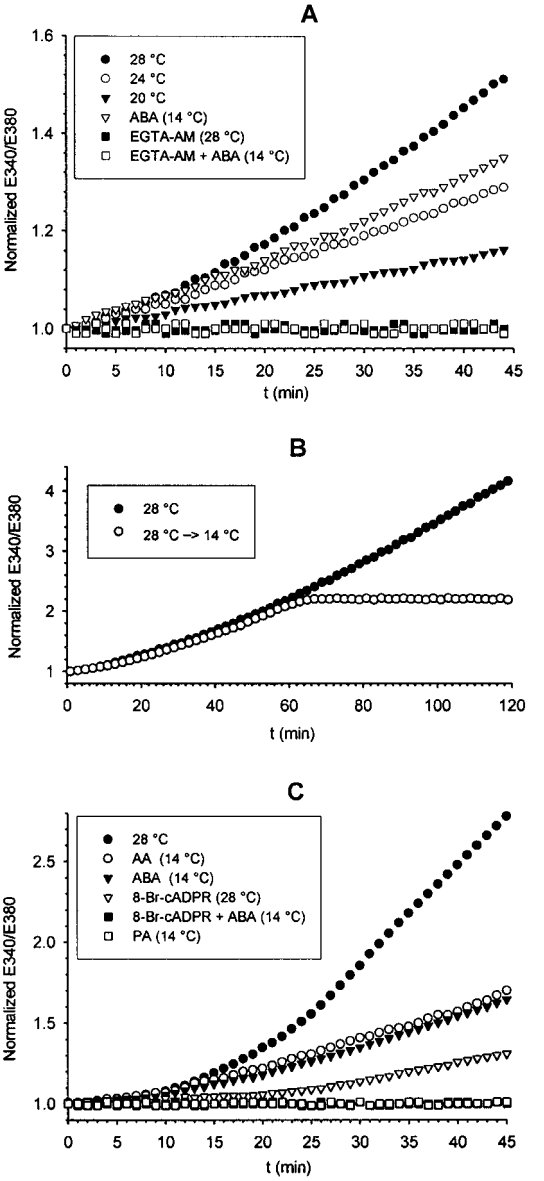

Fig. 1. Effect of temperature, ABA, and AA on $[Ca^{2+}]_i$ in *A. polypoides* cells. Fura 2-loaded cells were incubated in CMF-SW, or SW, containing 10 mM glucose at the indicated temperatures in a thermostated microfluorimetric cuvette, under continuous slow stirring. The fluorescence emission ratio E340/E380 (R) is shown. Ratios were acquired every 0.5 s. Each point is the mean of 120 acquisitions. Traces were normalized to a zero-time R of 1.0 to facilitate comparison. (*A*) Temperature dependence of the R increase and effect of ABA. Incubations were performed in CMF-SW. ABA was added at time = zero. Traces are from one of five comparable experiments, performed on different animals. (*B*) Traces from two representative experiments showing the increase of the $[Ca^{2+}]_i$ as continuously recorded over 2-h exposure of the cells to 28°C or 28°C for 60 min, followed by 14°C for the rest of the recording time. (*C*) Inhibition of the temperature- and ABA-induced increase of $[Ca^{2+}]_i$ by 8-Br-cADPR and effect of AA on $[Ca^{2+}]_i$. Fura 2-loaded cells were preincubated for 30 min at 14°C in SW with 20 μM 8-Br-cADPR, then washed, resuspended in SW, and exposed to 28°C in the cuvette. AA or palmitic acid (PA), both 50 μM, were added at time = zero to Fura-loaded cells at 14°C.

Heat Stress Stimulates ABA Production in *A. polypoides*. The effect of exogenously added ABA on cyclase activity of *A. polypoides* cells prompted us to investigate whether this phytohormone was present in sponge tissue. Indeed, ABA was detected in extracts from *A. polypoides* fragments, both by HPLC and ELISA, at 4.1 ± 1.5 pmol/g wet tissue (n = 8). The two techniques yielded comparable

values for the same sample. Significantly, the amount of ABA present in sponge tissue increased rapidly after exposure of *A. polypoides* to 26°C, from a basal value of 4.8 pmol/g to 18.1, 80.0, and 104.2 pmol/g after 60 sec, 5 min, and 60 min, respectively (results from a representative experiment). Thus, ABA generation by sponge cells proves to be downstream of temperature stress, its increased production inducing activation of ADP-ribosyl cyclase and the consequent increase of $[cADPR]_i$.

ABA Stimulates Cyclase Activation by Means of Protein Kinase A (PKA). Next, we investigated whether a kinase-dependent mechanism was involved in ABA-triggered cyclase activation, as observed in plants (21). The ABA-induced increase of the cyclase activity was completely prevented by addition of the protein kinase inhibitor K252a (1 μM) during incubation (Fig. 6*A*, which is published as supporting information on the PNAS web site). A similar effect also was afforded by K252a on the temperature-induced cyclase activation (not shown). Moreover, the cell-permeant PKA activator 8-Br-cAMP induced a marked (8-fold) increase of ADP-ribosyl cyclase activity on intact cells, whereas 8-Br-cGMP had only a minor effect (Fig. 6*A*). These results indicate that ABA induces cyclase activation by means of its PKA-dependent phosphorylation.

To obtain conclusive evidence for the role of phosphorylation on activation of ADP-ribosyl cyclase, we investigated the cyclase at a structural level on SDS/PAGE. To this purpose, we took advantage of the fact that ADP-ribosyl cyclase activity can be detected on mildly denaturing SDS/PAGE by way of its production of fluorescent cyclic inosine diphosphate ribose from NHD^+ (11). Immunoaffinity purification on antiphosphoserine antibody-coated agarose of sponge cell lysates, prepared from ^{32}P-orthophosphate-labeled cells, yielded a 28-kDa band that increased both in activity (i.e., fluorescence intensity) and apparent molecular mass in the heat-stressed and ABA-treated samples, compared with control (Fig. 7*A*, which is published as supporting information on the PNAS web site). The increase of activity and apparent molecular mass both were prevented by preincubation of sponge tissue fragments with K252a (Fig. 7*A*). Finally, autoradiography of the immunopurified bands demonstrated radioactive labeling of the activated cyclase (Fig. 7*B*). The low phosphorylation state of the control (Fig. 7*B*, lane 1), which indeed enabled immunopurification of a detectable cyclase activity (Fig. 7*A*, lane 1), could represent the basal (unstimulated) condition or it could be caused by the brief mechanical stress exerted upon sponge tissue during dissociation of the cells. The slight increase of the apparent molecular mass of the bands from the treated samples compared with the control could result from multiple phosphorylations taking place upon heat- or ABA-triggered activation of the cyclase.

A Heat- and Mechano-Gated Cation Channel Triggers the Temperature-Signaling Cascade. Recently, the mammalian thermoreceptor involved in both peripheral and hypothalamic thermosensing has been demonstrated to be a heat- and mechano-gated K^+-channel (TREK-1) (22). Our serendipitous observation that the mechanical stress induced on dissociated cells by repeated centrifugations also resulted in cyclase activation (not shown) prompted us to investigate whether a similar cation channel was responsible for triggering the temperature-signaling cascade in *A. polypoides*. Both the mammalian and the *Aplysia californica* heat- and mechano-gated K^+ channels are opened by micromolar AA, which mimics mechanical activation by modifying the membrane curvature (23), while they are blocked by PKA-dependent phosphorylation, by micromolar Gd^{3+} (but not by millimolar Ba^{2+}) (24, 25) and by local anesthetics (e.g., bupivacaine, ref. 26). Thus, we investigated the effect of AA on cyclase activity and tested whether bupivacaine could reverse the temperature-induced cyclase activation. As illustrated in Fig. 6*B*, a brief incubation of intact *A. polypoides* cells with 50 μM AA, but not with saturated palmitic acid, induced a more than 4-fold increase of cyclase activity, which was completely prevented by addition of 50 μM Gd^{3+}. The temperature-induced activation of the cyclase also was prevented by Gd^{3+} and 1 mM bupivacaine (Fig. 6*B*). These results suggested that opening of a heat-activated and polyunsaturated fatty acid-activated cation channel could be the first event in the signal transduction pathway leading to cyclase activation. To ascertain the relative position of ABA and the cation channel in the signaling cascade, the effects of AA- and temperature-mediated channel activation on ABA synthesis were investigated. Both AA and heat stress induced a rapid increase of ABA concentration in intact cells, an effect that was completely abolished by pretreatment of the cells with Gd^{3+} or bupivacaine (see Fig. 8, which is published as supporting information on the PNAS web site). These results demonstrate that ABA generation is downstream of the cation channel activity.

The demonstrated responsiveness of permeabilized *A. polypoides* cells to exogenously added cADPR (see Fig. 6*B*), prompted us to investigate the effect of heat stress, AA, and ABA on the intracellular Ca^{2+} concentration ($[Ca^{2+}]_i$) of intact sponge cells. Exposure of freshly dissociated, Fura 2-loaded *A. polypoides* cells to increasing temperatures (20°C, 24°C, or 28°C) determined an immediate and temperature-dependent increase of the E340/E380 fluorescence ratio (Fig. 1*A*), which conversely kept constant in cells incubated at 14°C (not shown). The rate of the increase was proportional to the temperature rise. If the temperature was lowered again from 28°C to 14°C 60 min after the onset of heat stress the increase of the fluorescence slowed down and ceased but the $[Ca^{2+}]_i$ remained elevated (Fig. 1*B*).

Addition of 50 nM ABA, at a constant temperature of 14°C, elicited a $[Ca^{2+}]_i$ increase comparable to that induced by a 10°C increase of temperature (Fig. 1*A*). Preincubation of the cells with 10 μM EGTA-AM, but not with 5 mM EGTA, completely prevented both the temperature- and ABA-induced increases of the E340/E380 ratio (Fig. 1*A*), demonstrating that the fluorescence signal was indeed originated by release of intracellular calcium. Qualitatively similar results also were obtained with an intracellular calcium imaging system (not shown). In this case, freshly dissociated, Fura 2-loaded sponge cells were allowed to reaggregate on polyornitine-covered glass coverslips in a 200-μl thermostated chamber and images from small (8–10) cell aggregates were acquired.

To investigate the role of cADPR in the temperature- and ABA-triggered increase of $[Ca^{2+}]_i$, we preincubated *A. polypoides* cells with 20 μM 8-Br-cADPR, a membrane-permeant cADPR antagonist (27), before exposure to high temperature or ABA. 8-Br-cADPR prevented the intracellular calcium increase in both cases (Fig. 1*C*), demonstrating a causal role of cADPR as the intracellular calcium mobilizer. Inhibition of the ABA-induced $[Ca^{2+}]_i$ increase also was obtained by addition of protein kinase inhibitor K252a (1 μM), confirming the involvement of a protein kinase in the signaling events leading to cyclase activation in response to ABA (not shown). These results demonstrate that calcium mobilization is downstream of both temperature- and ABA-triggered, cADPR-mediated signaling.

Finally, AA (10 μM), but not palmitic acid, also induced an intracellular calcium release similar to that obtained with ABA, indicating that mechano-activation of the cation channel by modification of the cell membrane curvature eventually results in a $[Ca^{2+}]_i$ increase. A similar effect also was observed with 10 μM lysophosphatidyl choline (C14:0) (not shown).

From the results described above, the following temperature-signaling pathway emerges in *A. polypoides*: a heat- (and mechano-) gated cation channel is opened and the $[ABA]_i$ increases, leading to PKA-mediated cyclase activation by means of phosphorylation, with the consequent increase of $[cADPR]_i$ and $[Ca^{2+}]_i$.

The Thermoreceptor of *A. polypoides* Is a Heat-Activated and Polyunsaturated Fatty Acid-Activated Cation Channel. To further verify the presence of a thermosensing cation channel on *A. polypoides*

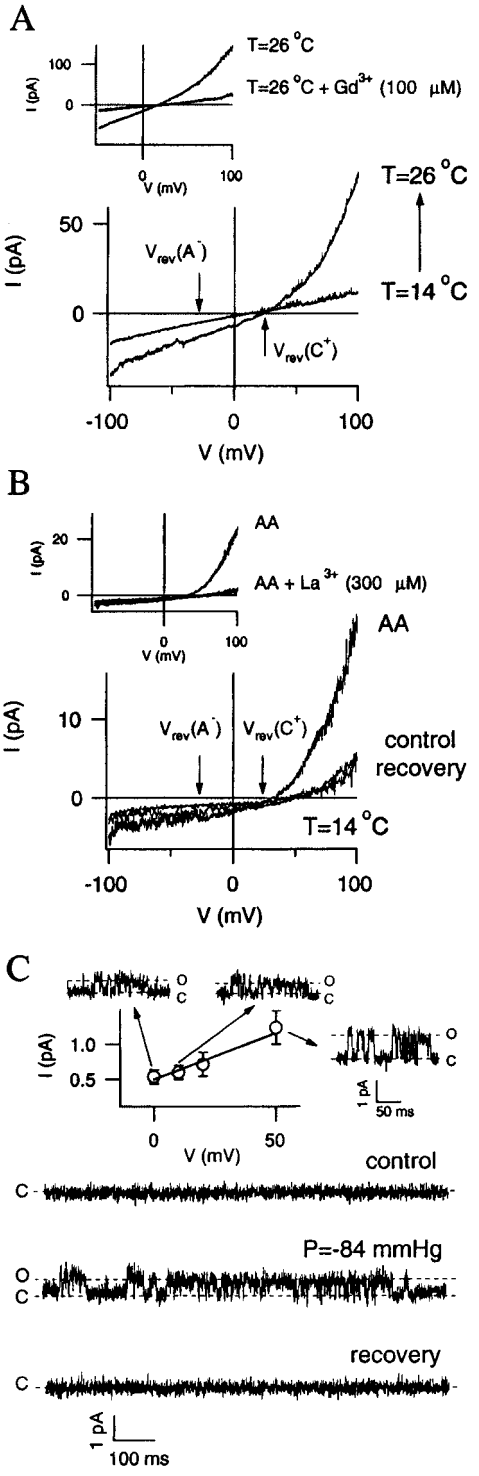

Fig. 2. Patch-clamp recording of transmembrane currents in *A. polypoides* cells. (*A*) Voltage ramps of 5-s duration were applied from a holding potential of −20 mV in whole-cell configuration. Currents were recorded at 14°C and 26°C, as indicated. Sampling and filtering frequencies were 2 and 0.5 KHz, respectively. Cells were bathed with external artificial SW and internal IntA solution. The arrows show the monovalent cationic [$V_{rev}(C^+)$ caused by Na^+ and K^+] and anionic [$V_{rev}(A^-)$ caused by Cl^-] reversal potentials, as calculated for the bathing and internal solutions in use. (*Inset*) The inhibition of the high temperature-induced current by 100 μM Gd^{3+}. (*B*) Currents recorded before, during, and after application of AA (100 μM), at $T = 14$°C under the same experimental conditions as in *A*. (*Inset*) The inhibition of the AA-induced current by 300 μM La^{3+}. (*C*) Single-channel recording of mechanical stress-activated channels in cell-attached configuration. Channel activity was recorded at atmospheric pressure and during stretch of −84 mmHg applied through the recording pipette ($V_m = 20$ mV), at 4-KHz sampling and 1-KHz filtering frequencies. Cells were bathed with external artificial SW and IntB solution into the pipette. (*Inset*) The single-channel *I–V* relationship and some example traces, measured at the minimum stretch needed to elicit the current. Each point has been evaluated from at least 50 single-channel transitions, and bars show the SEM. The channel conductance calculated from the best fit was 13 ± 4 pS.

cells and ascertain its role in the heat-signaling cascade, we investigated $^{86}Rb^+$ efflux from ^{86}Rb-loaded *A. polypoides* cells under conditions known to either activate or block heat- and mechanogated K^+ channels (22, 23, 25). $^{86}Rb^+$ efflux is a widely used experimental approach to analyze the properties of polyunsaturated fatty acid-activated K^+ channels (16). $^{86}Rb^+$ efflux, indicative of channel opening, was stimulated ≈2- and 5-fold, compared with control, by exposure of preloaded cells to heat stress (28°C) or 50 μM AA (14°C), respectively (Fig. 9*A*, which is published as supporting information on the PNAS web site). This increase of Rb^+ efflux was completely prevented by 50 μM Gd^{3+}, or La^{3+}, but not by 1 mM Ba^{2+}. The protein kinase inhibitor K252a increased $^{86}Rb^+$ efflux at both 14°C and 28°C, indicating that phosphorylation down-modulates the channel at 14°C and is also responsible for a "feedback" inhibition of heat-induced channel activation (Fig. 9*B*). The inhibitory effect on temperature-stimulated $^{86}Rb^+$ efflux exerted by 8-bromo-cAMP identifies PKA as the kinase involved in channel regulation.

Next, electrophysiological evidence for the presence of a heat-sensitive and mechanical stress-sensitive cation channel in *A. polypoides* was sought. Patch-clamp measurements on sponge cells had never been reported before and proved to be technically demanding. Presence of a heat-sensitive current in whole-cell configuration is shown by the current-voltage (*I—V*) curves in Fig. 2*A*. A rise in temperature from 14°C to 26°C induced an increase of the current that showed a strong outward rectification. The reversal potential of the current induced by heat was 23 ± 4 mV ($n = 3$), suggesting, in our experimental conditions, a monovalent cationic conductance. The effect of temperature was inhibited by Gd^{3+} (100 μM), as shown in the *Inset* of Fig. 2*A*. Similar results were obtained by perfusion of cells with 100 μM AA, under the same experimental conditions (Fig. 2*B*). The reversible, outwardly rectifying, AA-induced current showed a comparable reversal potential (28 ± 4 mV, $n = 3$) as the heat-induced current and was similarly inhibited by trivalent cations (Fig. 2*B Inset*). Moreover, mechanical stress-sensitive channels were observed in cell-attached configuration (Fig. 2*C*). Single channel activity, negligible at low temperature under normal pressure conditions, was strongly and reversibly increased by negative pressure-induced membrane stretch. The single channel conductivity, calculated from the *I–V* relationship (Fig. 2*C Inset*), was 13 ± 4 pS.

Taken together, these results indicate that *A. polypoides* cells express a heat-activated and mechanical stress-activated cation channel sharing pharmacological and regulatory properties with the mammalian and the *Aplysia* S-like K^+ channels (24, 25, 28, 29).

Summarizing all of the experimental data detailed above, the complete temperature-signaling cascade in *A. polypoides* can thus be outlined as shown in Fig. 3.

An interesting feature of this pathway is the feedback inhibition of the channel by means of PKA-mediated phosphorylation. This should limit the extent of the cADPR-induced calcium release after heat stress: indeed, the increase of $[Ca^{2+}]_i$ in response to a continuous temperature rise, as followed over a time span of several hours, could be fitted by a calculated sigmoidal curve (not shown). However, if the heat stress was prolonged for ≥4 h, a second "long-term" $[Ca^{2+}]_i$ increase followed the first one, reaching its maximal value 20 h after exposure of the cells to 26°C. Although addition of extracellular EGTA did not influence the short-term increase, it prevented the subsequent one (not shown). Therefore,

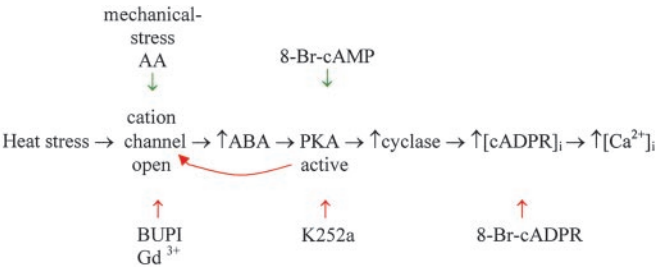

Fig. 3. The temperature-signaling cascade in *A. polypoides*.

the second "long-term" $[Ca^{2+}]_i$ increase is caused primarily by influx of Ca^{2+} from the extracellular space, possibly through Ca^{2+}-activated Ca^{2+} channels (30). The marked perturbation of the intracellular calcium homeostasis that follows negatively affects sponge cell protein synthesis and viability (not shown). Accordingly, these results may also provide insight into the biochemical mechanisms underlying the recently described mass-mortality episode involving sponges (among other epibenthic organisms), which occurred in September 1999 in the Northwestern Mediterranean Sea. An exceptional increase of the water temperature, which was recorded in different locations to be above 20°C (up from the normal value of ≅14°C) in the whole water column down to 40 m depth, has been advocated as a major factor inducing the massive die-off (31).

A striking feature of the signaling pathway described here is the long-lasting effect of even a transient temperature rise on the $[Ca^{2+}]_i$ in *A. polypoides*. This may be caused in part by the low cADPR hydrolase activity displayed by the sponge cyclase, ensuring a long half-life of the cADPR molecule, which is intrinsically resistant to nucleotidases and pyrophosphatases (6). A persistent perturbation of the $[Ca^{2+}]_i$ homeostasis is similarly observed upon induction of cADPR synthesis in cyclase negative murine 3T3 fibroblasts by transfection with the mammalian cyclase CD38 (6), although this protein has a cyclase to hydrolase ratio several orders of magnitude lower compared with the sponge enzyme. A second reason for the long-lasting $[Ca^{2+}]_i$ increase induced by heat stress in sponge cells is the extracellular Ca^{2+} influx that follows the initial Ca^{2+} release from intracellular stores. In essence, this mechanism provides a sort of cell "memory" by means of the $[Ca^{2+}]_i$, which could affect cell physiology long after the return of temperature to lower values. It is tempting to speculate that this heat- and mechano-activated cation channel and the signaling cascade it triggers may be the ancient precursors of the more complex forms of cell "learning" (presynaptic facilitation) present in *Aplysia* and involving a K^+ channel with similar properties (28).

Finally, the versatility of the cation channel thermoreceptor involved in the sponge-signaling cascade should be underscored: mechanical as well as thermal stimulations of this channel are demonstrated to result in an eventual increase of the intracellular concentration of free Ca^{2+}, whose role as the most versatile intracellular messenger is being established through the course of evolution (32). Mechano- and temperature-gated background K^+ channels have been implicated in various important "sensorial" functions in mammalian neuronal cells, including heat-, mechano-, intracellular pH-, and oxygen-sensing (22–25). The same kind of stimuli (water temperature, water movement and the consequent mechanical stimulation, intracellular pH and oxygen concentration in the water) are known to greatly affect sponge physiology (33). The fact that all these stimuli eventually may result in a cADPR-induced $[Ca^{2+}]_i$ increase suggests an ancestral role of cADPR as an intracellular signal relating cell functions to environmental conditions in a common progenitor of modern Metazoa. Indeed, involvement of ABA and cADPR in the signaling cascade triggered by environmental stress has been recently described in plants. Drought-induced ABA production has been shown to increase the $[cADPR]_i$ and the consequent increase of $[Ca^{2+}]_i$ in turn activates gene transcription (21) and reduces stomatal opening (34).

Interestingly, ABA has been detected in the brain of vertebrates (14), its function still unknown, its mere presence indeed a distant evolutionary heritage.

We are indebted to Prof. A. De Flora for advice and critical review of the manuscript and Dr. F. Gambale for helpful comments on the electrophysiological results. This work was supported by grants from the Consiglio Nazionale delle Ricerche, Target Project on Biotechnology, Ministero dell'Universitá e della Ricerca Scientifica e Tecnologica– Progetti di Rilevante Interesse Nazionale 2000, Ministero dell'Universitá e della Ricerca Scientifica e Tecnologica–Consiglio Nazionale delle Ricerche (5% Program on Biotechnology, l. 95/95), and Associazione Italiana per la Ricerca sul Cancro.

1. Masuda, W., Takenaka, S., Tsuyama, S., Tokunaga, M., Inui, H. & Miyatake, K. (1997) *FEBS Lett.* **405,** 104–106.
2. Lee, H. C. (1997) *Physiol. Rev.* **77,** 1133–1164.
3. Lee, H. C. (1994) *Cell. Signalling* **6,** 591–600.
4. Lee, H. C. (1996) *Biol. Signals* **5,** 101–110.
5. Takasawa, S., Nata, K., Yonekura, H. & Okamoto, H. (1993) *Science* **259,** 370–373.
6. Zocchi, E., Daga, A., Usai, C., Franco, L., Guida, L., Bruzzone, S., Costa, A., Marchetti, C. & De Flora, A. (1998) *J. Biol. Chem.* **273,** 8017–8024.
7. Rodrigo, A. G., Bergquist, P. R., Bergquist, P. L. & Reeves, R. A. (1994) in *Sponges in Time and Space*, eds. van Soest, R. W. M. & van Kempen, T. M. G. (Balkema, Rotterdam), pp. 47–54.
8. New, D. C. & Wong, J. T. (1998) *Biol. Signals Recept.* **7,** 98–108.
9. Pomponi, S. A. & Willoughby, R. (1994) in *Sponges in Time and Space*, eds. van Soest, R. W. M., van Kempen, T. M. G. & Braekman, J. C. (Balkema, Rotterdam), pp. 395–400.
10. Guida, L., Franco, L., Zocchi, E. & De Flora, A. (1995) *FEBS Lett.* **368,** 481–484.
11. Ziegler, M., Jorcke, D., Zhang, J., Schneider, R., Klocker, H., Auer, B. & Schweiger, M., *et al*. (1996) *Biochemistry* **35,** 5207–5212.
12. Podestà, M., Zocchi, E., Pitto, A., Usai, C., Franco, L., Bruzzone, S., Guida, L., Bacigalupo, A., Scadden, D., Walseth, T., *et al*. (2000) *FASEB J.* **14,** 680–690.
13. Franco, L., Zocchi, E., Usai, C., Guida, L., Bruzzone, S., Costa, A. & De Flora, A. (2001) *J. Biol. Chem.* **276,** 21642–21646.
14. Le Page-Degivry, M.-Th., Bidard, J.-N., Rouvier, E., Bulard, C. & Lazdunski, M. (1986) *Proc. Natl. Acad. Sci. USA* **83,** 1155–1158.
15. Heffetz, D., Fridkin, M. & Zick, Y. (1991) *Methods Enzymol.* **201,** 44–53.
16. Maingret, F., Fosset, M., Lesage, F., Lazdunski, M. & Honorè, E. (1999) *J. Biol. Chem.* **274,** 1381–1387.
17. Carpaneto, A., Cantu', A. M. & Gambale, F. (2001) *Planta* **213,** 457–468.
18. Munshi, C., Thiel, D. J., Mathews, I., Aarhus, R., Walseth, T. F. & Lee H. C. (1999) *J. Biol. Chem.* **274,** 30770–30777.
19. Graeff, R. M., Franco, L., De Flora, A. & Lee H. C. (1998) *J. Biol. Chem.* **273,** 118–125.
20. Graeff, R. M., Walseth, T. F., Hill, H. K. & Lee H. C. (1996) *Biochemistry* **35,** 379–386.
21. Wu, Y., Kuzma, J., Marechal, E., Graeff, R., Lee, H. C., Foster, R. & Chua, N. H. (1997) *Science* **278,** 2126–2130.
22. Maingret, F., Lauritzen, I., Patel, A. J., Heurteaux, C., Reyes, R., Lesage, F., Lazdunski M. & Honorè, E. (2000) *EMBO J.* **19,** 2483–2491.
23. Maingret, F., Patel, A., Lesage, F., Lazdunski, M. & Honorè, E. (2000) *J. Biol. Chem.* **275,** 10128–10133.
24. Maingret, F., Patel, A., Lesage, F., Lazdunski, M. & Honorè, E. (1999) *J. Biol. Chem.* **274,** 26691–26696.
25. Patel, A., Honorè, E., Maingret, F., Lesage, F., Fink, M., Duprat, F. & Lazdunski, M. (1998) *EMBO J.* **17,** 4283–4290.
26. Kindler, C. H., Yost, C. S. & Gray, A. T. (1999) *Anesthesiology* **90,** 1092–1102.
27. Walseth, T. F. & Lee, H. C. (1993) *Biochim. Biophys. Acta* **1178,** 235–242.
28. Klein, M., Camardo, J. & Kandel E. R. (1982) *Proc. Natl. Acad. Sci. USA* **79,** 5713–5717.
29. Shuster, M. J., Camardo, J. S., Siegelbaum, S. A. & Kandel, E. R. (1985) *Nature (London)* **313,** 392–395.
30. Reichling, D., B. & Levine, J. D. (1997) *Proc. Natl. Acad. Sci. USA* **94,** 7006–7011.
31. Cerrano, C., Bavestrello, G., Nike, Bianchi, C., Cattaneo-Vietti, R., Bava, S., Morganti, C., Morri, C., Picco, P., Sara, G., Schiapparelli, S., *et al*. (2000) *Ecol. Lett.* **3,** 284–293.
32. Carafoli, E., Santella, L., Branca, D. & Brini, M. (2001) *Crit. Rev. Biochem. Mol. Biol.* **36,** 107–260.
33. Sarà, M. & Vacelet, J. (1973) *Ecologie de Démosponges*, ed. Grassé, P. P. (Anatomie Systematique, Biologie, Masson, Paris), pp. 462–576.
34. Leckie, C. P., McAinsh, M. R., Allen, G. J., Sanders, D. & Hetherington, A. M. (1998) *Proc. Natl. Acad. Sci. USA* **95,** 15837–15842.